JOURNAL OF PROPULSION AND POWER
Vol. 24, No. 4, July–August 2008

Passive Control Techniques to Alleviate Supersonic Cavity Flow Oscillation

Youngki Lee*
Poongsan Company, Chungnam 320-822, Republic of Korea
Minsung Kang† and Heuydong Kim‡
Andong National University, Gyeongbuk 760-749, Republic of Korea
and
Toshiaki Setoguchi§
Saga University, Saga 840-8502, Japan

DOI: 10.2514/1.30292

The effectiveness of two passive control techniques for alleviating the pressure oscillation generated in a supersonic cavity flow was investigated numerically. The control devices suggested in the present study include a triangular bump and a subcavity installed near the leading edge of a rectangular cavity. Time-dependent supersonic cavity flow characteristics with turbulent features were examined by using the three-dimensional, mass-averaged Navier–Stokes computation based on a finite volume scheme and large eddy simulation. The results show that the pressure oscillation near the trailing edge dominates overall time-dependent cavity pressure variations. Such an oscillation can be attenuated more significantly in the presence of the subcavity compared with the bump or blowing, and a larger subcavity leads to better control performance.

Nomenclature

C_p	=	pressure coefficient
D	=	depth of cavity
f	=	frequency
L	=	length of cavity
M	=	Mach number
Re_{unit}	=	unit Reynolds number
t	=	time
t'	=	time normalized by the period for a dominant frequency
U	=	mean velocity
W	=	width of cavity
x	=	longitudinal distance
ρ	=	density

Subscripts

0	=	total state
i	=	incoming flow
j	=	blowing jet
s	=	subcavity

Introduction

THE research on the noise and oscillation generated in a cavity flow activated in the 1950s [1] has been carried out with regard to a variety of issues motivated by the rapid growth of the global aerospace industry over the years. Past studies in this research field focused mainly on understanding the effects of a change in the depth or length of the cavity on cavity flow characteristics at a given mean velocity of main flow [2] and developing an optimum method to solve a specific problem in consideration of specific cavity flow conditions and characteristics [3]. Despite the geometrical simplicity, the complicated physics resulting from the generic unsteadiness of viscous-inviscid flow interaction and flow-acoustic interaction occurring in a feedback mechanism [4] are not easy to solve because these are strongly dependent on upstream conditions and cavity geometry [5]. Numerous solution approaches [6–8] have therefore been developed with different accuracy levels to meet the specific requirements of particular applications.

The research of supersonic cavity flow was motivated by the development of the weapons bay for stealth aircraft designed to absorb and deflect radio waves in the 1980s [9]. As a cavity system is exposed to a supersonic stream, an intense pressure oscillation generated in the cavity flow can lead to buffeting, acoustic fatigue, and additional drag, and the unsteady flow characteristics are significantly different from those at subsonic speeds [10]. A typical supersonic cavity flow over a closed cavity [11] includes a shear layer generated from the leading edge of the cavity, a recirculation within the cavity, an oblique shock wave induced by the shear layer near the leading edge, and a bow shock/expansion wave system generated ahead of the trailing edge of the cavity, as shown in Fig. 1. The inherent unsteadiness of the cavity flow is concerned principally with a time-dependent variation of the shear layer structure, which leads to a significant change in the wave interaction with the shear layer and cavity walls and recirculation characteristics in the cavity. The aims of the studies in this speed range have therefore mainly been predicting properly and minimizing the harmful flow features to enhance flight stability and efficiency.

Generally, a feedback mechanism decides unsteady cavity flow characteristics that a free shear layer separated from the leading edge impinges on the trailing edge, generating acoustic waves that propagate upstream and further excite the shear layer growth [12]. Because the mechanism differs from one flow regime to the other for a given cavity system, a number of active and passive control techniques have been suggested to satisfy the control performance for a particular case. Typical control methods posited to date are summarized in Table 1.

Many active control techniques have adopted mass blowing of highly compressed air or an actuator in front of the leading edge or on

Received 5 March 2007; revision received 27 February 2008; accepted for publication 29 February 2008.

*Manager, Defense Product Technical Research Laboratory, Nonsan; yklee@poongsan.co.kr.
†Postgraduate Student, School of Mechanical Engineering, Andong; hahakang@anuis.andong.ac.kr.
‡Professor, School of Mechanical Engineering, Andong; kimhd@andong.ac.kr. Member AIAA.
§Professor, Department of Mechanical Engineering, 1, Honjo-machi,; setoguci@me.saga-u.ac.jp.

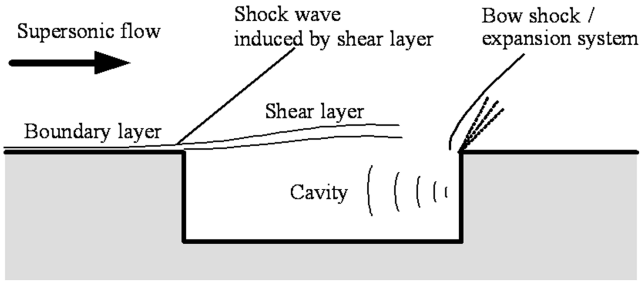

Fig. 1 Supersonic cavity flow.

the bottom of cavity to manipulate the receptivity of the boundary layer approaching the cavity or to weaken the excitation of the shear flow by radiated pressure waves within the cavity [13]. Compared with passive control, this type of control can offer better performance for a wider range of flow conditions but requires additional weight and cost due to the supplementary devices used to produce energy for blowing, such as a chamber-nozzle system and moving parts. For this reason, though passive control is generally known to be limited by particular flow conditions, its handiness has recently appealed to many researchers and engineers for the development of devices less sensitive to the flow Mach number and cavity type.

The ultimate requirements of cavity control are to be cost effective, easy to install, applicable to various flow conditions, and harmless to the system performance. To date, no techniques have been reported to satisfy these conditions totally, and the latest research has focused on this issue. As the first step to achieving this goal, the present paper addresses the effectiveness of two passive means, a triangular bump and a subcavity placed near the leading edge for the pressure oscillation control of a supersonic cavity flow. The authors' work seeks to provide proof of applicability to various cavity flows using computational and experimental methods.

The majority of studies regarding cavity flow with and without control have been conducted through surface pressure measurements with simple visualization [21–24] or two-dimensional numerical simulation [25–27], which can hardly provide insight into the detailed cavity flow mechanism or the proper prediction of the noise level. Full three-dimensional computation is therefore indispensable to overcome the difficulties. A detailed feedback mechanism and the turbulent features of a Mach 1.8 supersonic flow with a closed cavity were examined by the three-dimensional unsteady Navier–Stokes computation and a large eddy simulation (LES) and validated with some results of our wind-tunnel tests.

Methodology

Testing Model

Figure 2 shows the schematic description of the cavity model and flow control devices considered in the present computation. A rectangular cavity installed in a rectangular duct with a height of 20 mm has a depth (D) of 20 mm; its length (L) and width (W) are given as $2.0D$ and $1.8D$, respectively. The Mach number of the incoming flow (M_i) toward the cavity is 1.8 for all of the cases tested. The passive control devices adopted here to reduce the pressure oscillation generated in the cavity include a triangular bump and a subcavity. In the figure, the bump is designed as a bar type with a triangular cross section that has a height of $0.025D$, and its center is located 1.5 mm upstream of the leading edge of cavity. The subcavity is placed just 0.1 mm beneath the leading edge, and its depth is $1/3D$. Two different subcavity lengths (L_s), $1/3D$ and $2/3D$, are tested to verify the effect of L_s on the pressure oscillation reduction, which was studied by the authors previously using a two-dimensional computational fluid dynamics (CFD) method [28]. A blowing slit is also tested for the purpose of comparing the control performance with other passive methods. The location and scale of the slit are chosen based on the triangular bump setup. During the computation, time-dependent flow information, such as local wall static pressure and pressure spectra, is collected at location nos. 1, 2, and 3 as denoted in the figure.

Numerical Methods

In the present computation, a commercial computational code, FLUENT 6 [29], is adopted to understand a complex flow structure observed near a supersonic cavity, including various wave systems, vortices, strong shear layers, and their interactions. The three-dimensional, unsteady, mass-averaged Navier–Stokes equations governing the cavity flowfield are discretized spatially by an implicit finite volume scheme and temporally by a multistage Runge–Kutta scheme. LES using the Smagorinsky–Lilly model [30] has been performed to properly predict the turbulent features of the unsteady cavity flow. For better convergence and accurate solutions, the solution procedure includes the preconditioning treatment [31], which allows the propagation of acoustic waves in the system to be singled out. The details of the governing equations and solution procedures are given in Lee et al. [32].

In the implicit finite volume scheme involved in the present CFD code, the physical domain is subdivided into numerical cells, and the integral equations are applied to each cell. The flowfield is represented by associating a distinct value of the discretized solution vector with each control volume, which is then used to evaluate the fluxes at the cell faces. The solution vector is computed using a multidimensional linear reconstruction approach [33], which enables a higher-order accuracy to be achieved at the cell faces through a Taylor series expansion of the cell-averaged solution vector. The use of a second-order upwind scheme makes it feasible to capture the location and structure of the pressure waves, vortices, and shear flow generated around a cavity. With respect to the temporal discretization, an explicit multistage time-stepping scheme [34] is used to discretize the time derivatives in the governing equations.

Table 1 Active and passive cavity flow control methods

Type	Device	Effects and problems	References
Active control	Blowing: Continuous	1) Lifting of shear layer 2) Reduction in radiated waves 3) Optimum control location: below the leading edge 4) Requirement of large mass flux adding system weight	Lamp and Chokani [12] Rona and Brooksbank [13] Smith [14] Vakili and Gauthier [15]
	Blowing: Pulsed		
	Blowing: Perforated plate		
	Powered resonance tubes	1) Suppression of flow-induced resonance	Stanek et al. [16]
	Piezoelectric flap actuator	1) Suppression of cavity tone at the first mode 2) Involving moving parts with the risk of fatigue	Cattafesta et al. [17]
Passive control	Ramped trailing edge	1) Alleviation of the Rossiter modes	
	Spoiler at the leading edge	1) Lifting of shear layer 2) 15 dB reduction in sound pressure level (SPL) at $L/D = 4.5$ and $M = 0.95$	Baysal et al. [18]
	Compression ramp at the leading edge	1) Small reduction in SPL at $L/D = 3$ and $M = 1.5$–2.5	Zhang et al. [19]
	Leading-edge fence	1) Suppression of dynamic-pressure load	Ukeiley et al. [20]

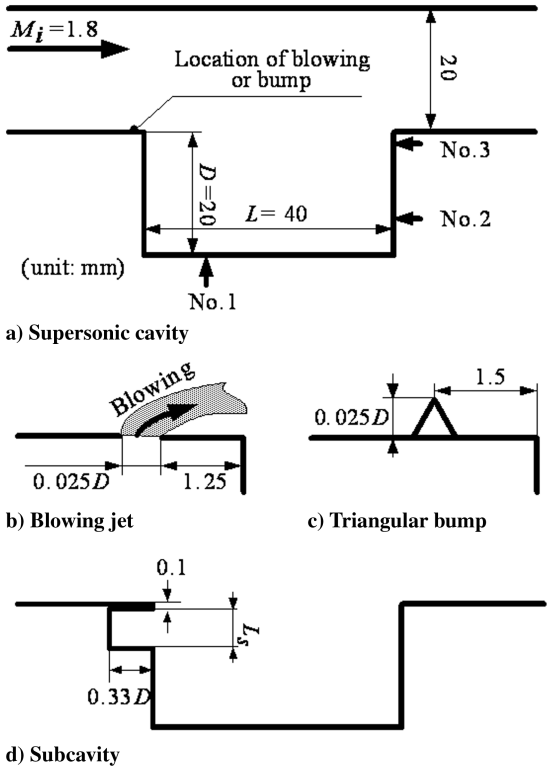

Fig. 2 Cavity model and control devices.

Computational Grids and Boundary Conditions

Figure 3 shows the computational domain with a structured grid system and the boundary conditions used in the computation without a control. The domain for the duct has a length of $4D$, which is built by $130 \times 45 \times 64$ hexahedral cells, and $70 \times 45 \times 65$ cells are used to create the cavity. Grids were clustered around the regions with a large pressure gradient, such as a shear layer, cavity edges, and shock waves, and about 600,000 nodes were applied in the cases without a control device and with a triangular bump. With a subcavity or a blowing slit, due to the additional grids required for the subcavity domain and the jet flow region in the duct, about 700,000 nodes were used in total.

Several grid sizes were tested and resulted in divergence or failure in the proper simulation of the self-oscillatory behavior of the cavity flow if they were insufficient. Even if a solution was converged at each time step during the time-dependent calculation, it never offered a physically correct result that could depict the unique flow unsteadiness unless an appropriate time-step size and iteration numbers at each time step were selected. With the present grid systems, a reasonable simulation of the self-oscillatory motions of the cavity flow could be completed using a time-step size of 0.5×10^{-8} s. The present grid systems are possibly not the best resolution. To prove the accuracy of the prediction, therefore, some solutions were validated with our experimental results, given in the next section.

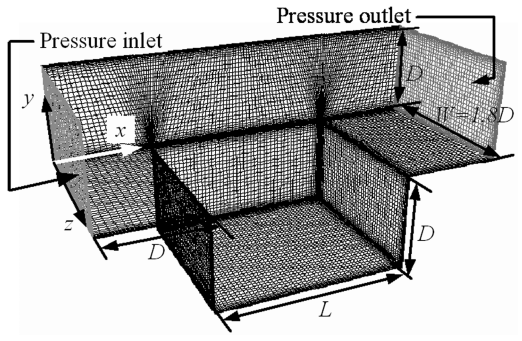

Fig. 3 Computational grids and boundary conditions without a control.

Regarding the boundary conditions, the total pressure and temperature (405 kPa and 293 K) are applied to the inlet boundary, and static pressure is applied to the outlet boundary. On the solid walls of the duct and cavity, no-slip and adiabatic conditions are applied. In the case using a blowing slit, the exit of the slit is defined as a mass flow inlet boundary, and the mass flow rate of the blowing jet is given by 0.0067 kg/s at $p_{j0} = 203$ kPa and $T_{j0} = 293$ K. During the computation, solutions were considered converged when the residuals of the mass, momentum, and energy equations dropped to 1.0×10^{-4} at each time step. With the convergence criteria, the mass imbalance was also monitored for flow inlet and outlet boundaries, and it was set to be less than $\pm 0.01\%$ of the incoming mass for converged solutions.

Results and Discussion

Validation

Steady-state solutions with the present CFD code were first validated with an experimental result obtained by Sakamoto et al. [35]. Figure 4 presents the surface pressure distributions along the centerline ($z/D = 0.9$) of a rectangular cavity at $L/D = 3.0$ and $M_i = 1.83$, and the experimental data are taken from a past wind-tunnel test [35]. In the figure, x/D is the nondimensional distance in the flow direction, and the wall pressure values are shown as the pressure coefficient C_p, defined by $(p - p_i)/(0.5\rho_i U_i^2)$. Both computed and measured distributions are very close, especially at the locations with high pressure due to an oblique shock wave near the leading edge ($x/D \sim 1$), the effect of the shear layer impingement on the rear wall of cavity ($x/D \sim 5$), and a bow shock/expansion system ($x/D \sim 6$). From Fig. 4, therefore, the present CFD code is considered relevant to obtaining a steady-state solution, which is used as an initial solution of time-dependent flow analyses.

The schematic diagram presented in Fig. 5 shows a supersonic cavity model with a subcavity ($L = D = 12$ mm) chosen to validate the present CFD code. In this case, the subcavity reaches the floor of the cavity, and unsteady pressure data are collected at a single point, P, which is located 3 mm below the trailing edge. This is because a dominant pressure oscillation is generated near the trailing edge, a fact that will be discussed in the following results. The pressure measurement was conducted using a suction-type supersonic wind tunnel with a test section of $40 \times 40 \times 38$ mm^3 and a Kulite XT-190 pressure transducer. The inlet total pressure and temperature are 101 kPa and 293 K, respectively, and the unit Reynolds number of incoming flow (Re_{unit}) is 4.2×10^7 m^{-1} at $M_i = 1.83$. As shown in Fig. 6, for both cases with and without a control, the computed results showed good agreement with the experimental ones. With the grid

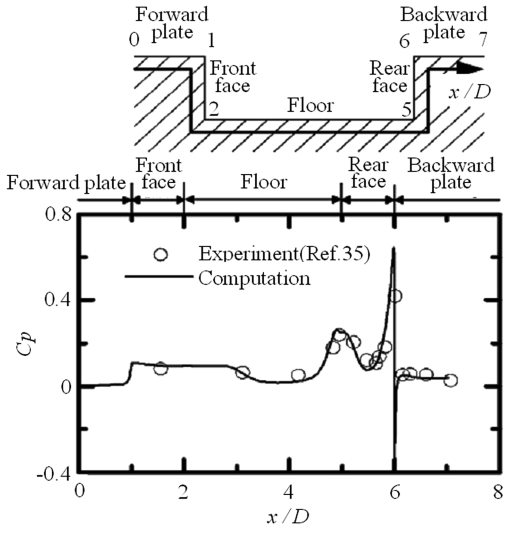

Fig. 4 Static pressure distributions ($L/D = 3.0$ and $M_i = 1.83$).

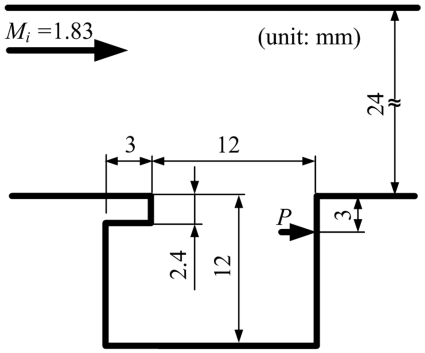

Fig. 5 Supersonic cavity model for the validation of the unsteady simulation ($L/D = 1.0$ and $M_i = 1.83$).

system and time-step size selected in the present computation, the CFD code predicts the dominant frequencies correctly with a small discrepancy in power spectrum density (PSD) value.

Unsteady Flow Without Control (Main Model)

Figure 7 shows a change in the flow structure over time with density and pressure contours to understand a periodical flow mechanism around the cavity without a control. In the figure, the nondimensional time t' is defined as the ratio of flow time to the period of the dominant frequency. About 11 kHz of dominant frequency are obtained from the result of the present case. At $t' = 0$, due to the shear layer impingement on the trailing edge of the cavity, a very high-pressure region is observed along the real wall, and intense pressure waves are generated. As time elapses, pressure waves propagate upstream within the cavity and lift the shear layer. During this situation, depending on low- and high-pressure regions of vortical flow inside the cavity, the shear layer is flapping, and the shock and expansion waves formed above the shear layer interact with each other complicatedly. At $t' = 1.02$, the influence of shear layer impingement is observed again. It is therefore considered that the present computation appropriately predicts a typical feedback mechanism leading to a periodical pressure oscillation of supersonic cavity flow.

Figure 8 shows static pressure variations occurring around the present cavity model ($L/D = 2.0$) for about one period, in which the longitudinal distance is normalized by the depth of cavity. Each distribution indicates that the most significant pressure rise is obtained at around $x/D = 5$, which is the location of the trailing edge. Over time, the wall pressure oscillates in the region of $x/D > 1$, and such a time-dependent variation is observed to be more severe between $x/D = 4$ and 5. It implies that an overall pressure oscillation of the cavity flow is dominated by the flow characteristics near the trailing edge, and the cavity flow control would rather be a way to manipulate the shear flow.

Cavity Flow Oscillation with and Without Passive Control

Figures 9 and 10 show the time histories of the static pressures obtained at predefined measuring points (see nos. 1, 2, and 3 in Fig. 2) on the cavity wall and their pressure spectra with and without a control. In the figures, the local wall static pressure is given as the values normalized by the total pressure p_0. Both results show that the most considerable pressure oscillation and the maximum peak $f \times$ PSD value occur at no. 3 for the all of the cavity models tested. In the presence of a triangular bump, the dominant frequency increases up to 14.7 kHz, compared with the no-control case. $(p/p_0)_{\max} - (p/p_0)_{\min}$ and the rms of pressure variations (Table 2) and the peak values of $f \times$ PSD increase at location nos. 1 and 2, whereas the values decrease at location no. 3 (e.g., about a 9.5% reduction in the rms of the pressure oscillation). As mentioned in Fig. 8, the effect of the pressure oscillation at location no. 3 dominates the overall cavity pressure oscillation. It can therefore be considered that the resulting level of pressure oscillation may decrease slightly, but the effectiveness of the control with the present bump configuration is not as obvious as that obtained by the use of blowing.

In Figs. 9d and 10, compared with other control methods, a subcavity ($L_s = 1/3D$) results in a relatively lower amplitude of pressure variations for all of the data acquisition points. The rms value is about 38% lower than that of the no-control case, and a reduction in $f \times$ PSD is clear at each location. The results can be attributed mainly to the interaction of vortical flows generated in the subcavity and main cavity. It is explained clearly through the flow visualization images shown in Fig. 11. Using a blowing jet, the pressure oscillation energy is concentrated mostly in a range under 15 kHz, and a considerable reduction in the pressure oscillation energy is observed only at no. 3 due to the decrease in frequency. As a result, the subcavity gave a better control performance compared with the other control methods tested in the present study.

Figure 11 shows the pressure contours with the corresponding velocity vectors obtained near a subcavity to examine a change in the cavity flow structure as time elapses. At $t = 0$ μs, a flapping shear layer instability and strong pressure waves are generated by the shear layer impingement on the rear wall. The high-pressure region propagating toward the leading edge and thus affecting shear layer

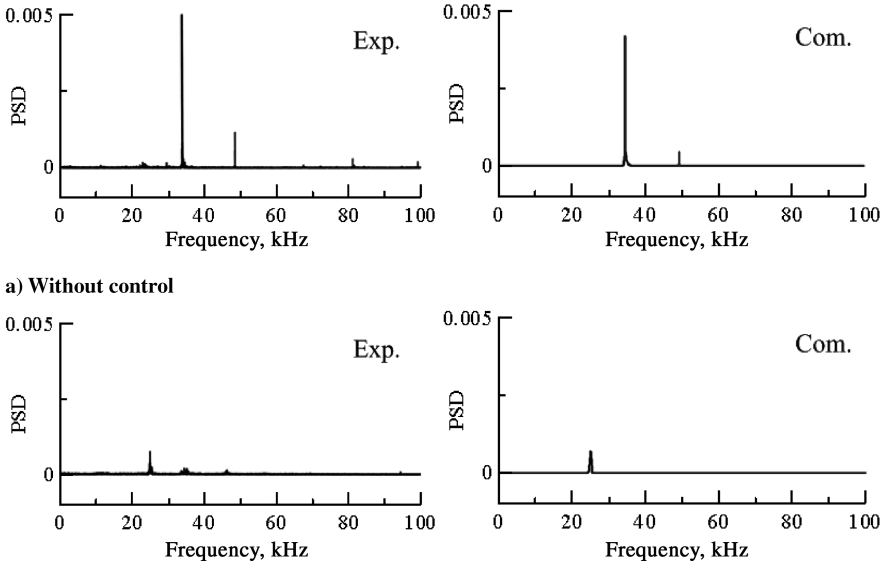

a) Without control

b) Subcavity (L_s=4/5D with a depth of 0.25D)

Fig. 6 Pressure spectra with and without a control.

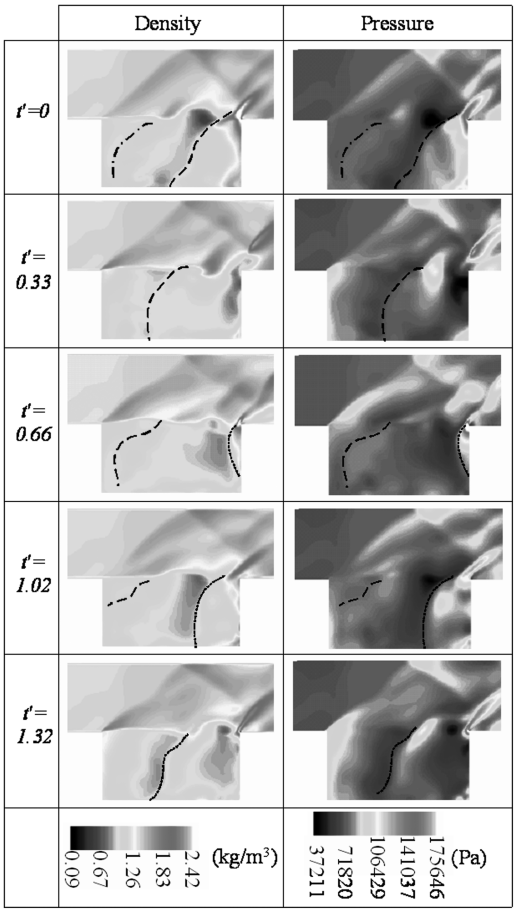

Fig. 7 Flow structure over time without a control in the x–y plane ($z/D = 0.9$).

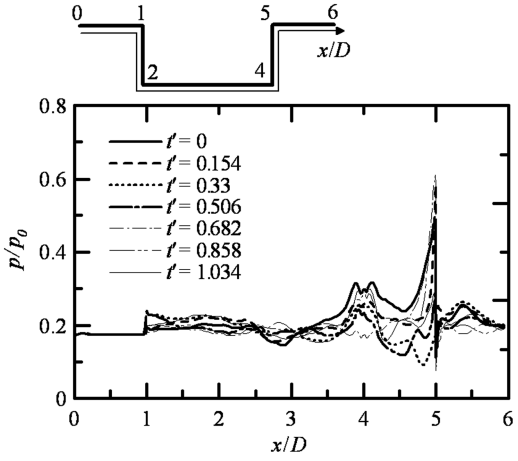

Fig. 8 Static pressure distributions along the cavity wall for about one period.

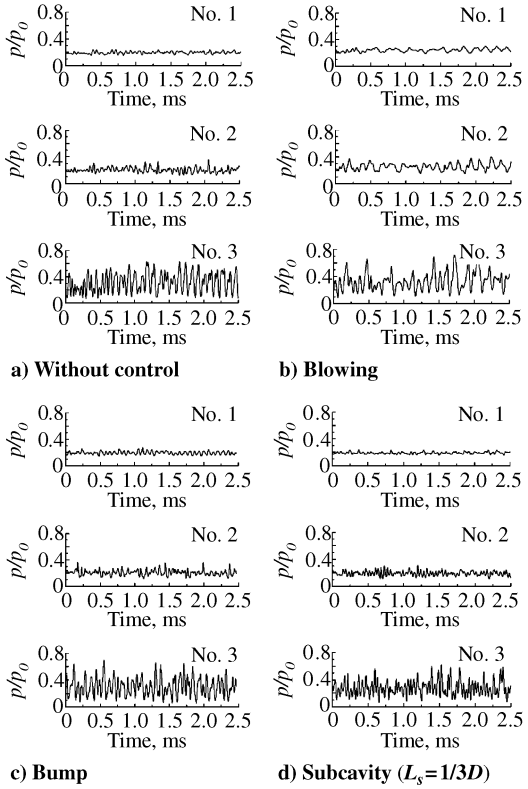

Fig. 9 Time histories of the cavity wall pressure with and without a control.

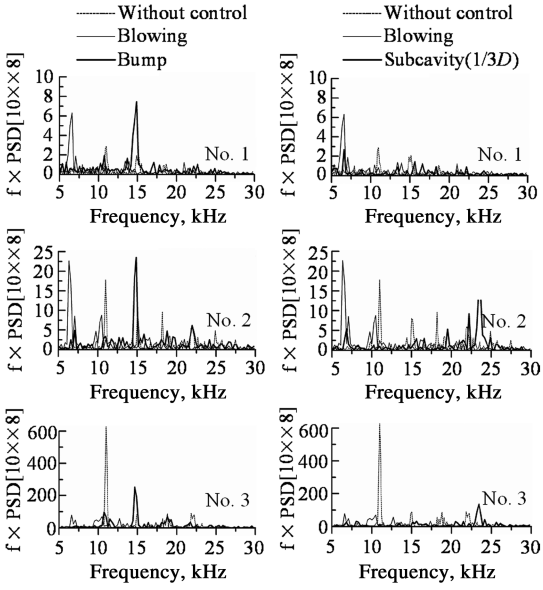

Fig. 10 Pressure spectra obtained on the cavity wall with and without a control.

development interacts with a vortical flow in the subcavity before it reaches to the shear layer. At $t = 20$ μs, the pressure around the leading edge of the cavity becomes very high due to the flow interaction, and some of the pressure waves are propagated into the subcavity. As time increases, the high-pressure flow moves back to the main cavity, and it interacts with the main cavity flow leading to strong vortices from the edge of the subcavity entrance. The high-pressure region along the shear layer propagates downstream and

Table 2 $(p/p_0)_{max} - (p/p_0)_{min}$ and rms of pressure variations with and without a bump

Position	No. 1		No. 2		No. 3	
Triangular bump	Without	With	Without	With	Without	With
$(p/p_0)_{max} - (p/p_0)_{min}$	0.081	0.134	0.233	0.242	0.56	0.634
RMS	0.0158	0.0212	0.0347	0.0356	0.1427	0.1291

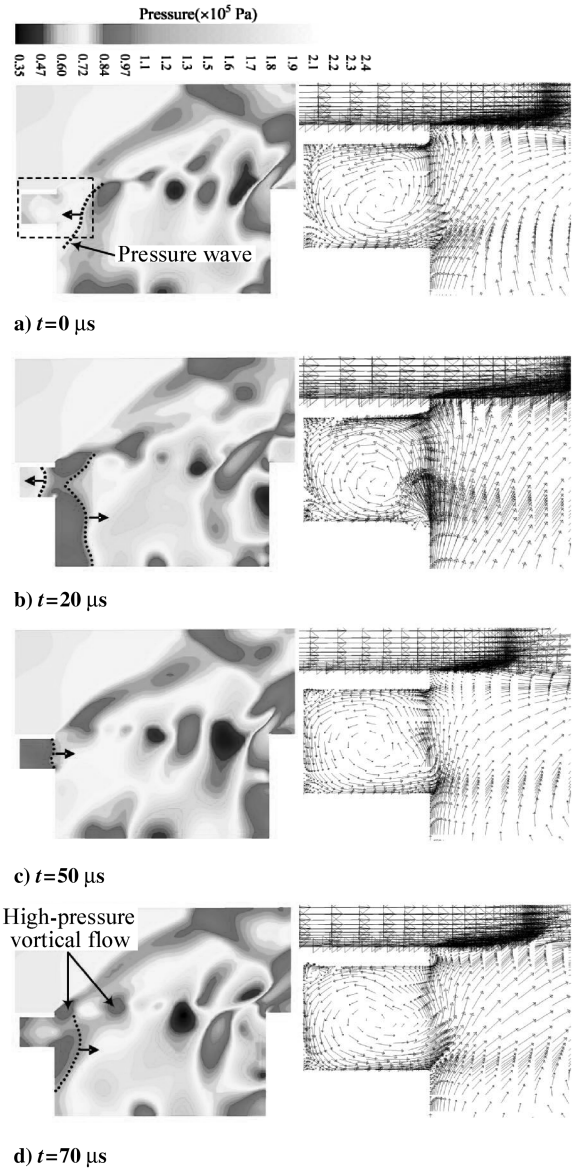

Fig. 11 Flow structures over time with a subcavity (*x–y* plane, $z/D = 0.9$, and $L_s = 1/3D$).

impinges on the rear wall, resulting in severe pressure oscillation. In this situation, the use of the subcavity changes the development of the vortex convection velocity in a way to weaken the impingement of the shear layer, though the frequency is somewhat increased (see Fig. 9).

Figure 12 shows the effect of the subcavity length on the pressure spectra, which indicates that a larger subcavity leads to a slightly reduced pressure oscillation energy. At $L_s = 2/3D$, pressure oscillation is observed to be insignificant at all of the locations tested in the entire frequency range. The effect of the control must be dependent on the volume of the cavity rather than on the length only. Therefore, further investigations are required regarding subcavity dimensions, namely, both the cavity length and depth and the location of the cavity measured from the leading edge.

Conclusions

The present study describes new passive control techniques of cavity flow oscillation using a triangular bump or a subcavity. The techniques are basically leading-edge control and the manipulation of shear layer development to alleviate the pressure oscillation of a supersonic cavity flow. A three-dimensional Navier–Stokes computation with LES was carried out for a Mach 1.8 of supersonic

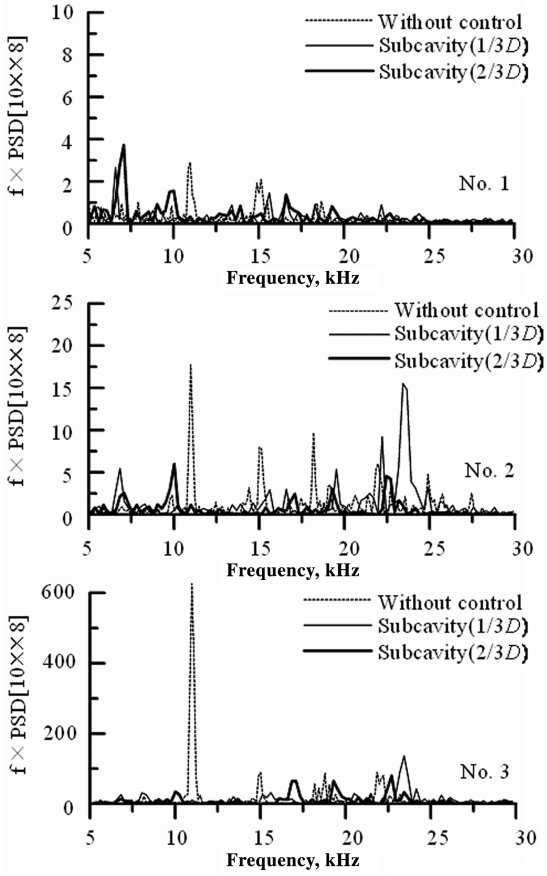

Fig. 12 Pressure spectra for the cases with a subcavity.

flow over a rectangular cavity. The present computational method was validated for both steady and unsteady solutions, and it was proved to be suitable for the simulation of the supersonic cavity flow under consideration.

The computational results showed that the pressure oscillation near the rear wall dominated the overall time-dependent cavity pressure variations. Using the present passive devices, a considerable reduction in the pressure oscillation energy could be obtained basically near the trailing edge, which means the attenuation of the main source of the pressure oscillation. A triangular bump was expected to function as mass blowing by lifting the shear layer in a similar way at the same location. However, the effectiveness of a triangular bump was not obvious for the current design. The results, especially, indicated that a subcavity can be a useful method for pressure oscillation control as its configuration is chosen properly. The influence of the subcavity length, that a longer subcavity gives reduced a pressure oscillation, was simulated clearly, and it is concluded that the influence needs to be examined simultaneously with that of the subcavity depth. Further research is therefore being carried out regarding cavity dimensions and the location and size of the bump to optimize control performance. To guarantee their controllability for various applications, the geometric parameters should be tested at a wide range of flow conditions.

Acknowledgment

This work was supported by the Korea Research Foundation Grant funded by the Korean Government (KRF-2007-D00060).

References

[1] Krishnamurty, "Sound Radiation from Surface Cutouts in High Speed Flow," Ph.D. Thesis, California Inst. of Technology, Pasadena, CA, 1956.

[2] Wilcox, F. J., Jr., "Experimental Measurements of Internal Store Separation Characteristics at Supersonic Speeds," *Proceedings of*

Conference on Store Carriage, Integration and Release, Royal Aeronautical Society, Bath, England, U.K., 1990, pp. 5.1–5.16.
[3] Hardin, J. C., and Pope, D. S., "Sound Generation by Flow Over a Two-Dimensional Cavity," *AIAA Journal*, Vol. 33, No. 3, 1995, pp. 407–412.
[4] Tam, C. K. W., and Block, P. J. W., "On the Tones and Pressure Oscillations Induced by Blow over Rectangular Cavities," *Journal of Fluid Mechanics*, Vol. 89, 1978, pp. 373–399. doi:10.1017/S0022112078002657
[5] Maull, D. J., and East, L. F., "Three-Dimensional Flow in Cavities," *Journal of Fluid Mechanics*, Vol. 16, 1963, pp. 620–632. doi:10.1017/S0022112063001014
[6] Borland, C. J., "Numerical Prediction of the Unsteady Flowfield in an Open Cavity," AIAA Paper 77-673, 1977.
[7] Gloerfelt, X., Bailly, C., and Juvé, D., "Computation of the Noise Radiated by a Subsonic Cavity Using Direct Numerical Simulation," AIAA Paper 2001-0226, 2001.
[8] Arunajatesan, S., and Sinha, N., "Unified RANS–LES Simulations of Cavity Flow Fields," AIAA Paper 2001-0516, 2001.
[9] Cattafesta, L., Shukla, D., Garg, S., and Ross, J., "Development of an Adaptive Weapons-Bay Suppression System," AIAA Paper 1999-1901, 1999.
[10] Block, P. J. W., "Noise Response of Cavities of Varying Dimensions at Subsonic Speeds," NASA TN D-8351, 1976.
[11] Rossiter, J., "Wind-Tunnel Experiments on the Flow over Rectangular Cavities at Subsonic and Transonic Speeds," Aeronautical Research Council, Rept. 3438, 1964.
[12] Lamp, A., and Chokani, N., "Control of Cavity Resonance Using Steady and Oscillatory Blowing," AIAA Paper 1999-0999, 1999.
[13] Rona, A., and Brooksbank, E. J., "Injection Parameters for an Effective Passive Control of Cavity Flow Instability," AIAA Paper 2002-0119, 2002.
[14] Smith, B. R., "Computational Simulation of Active Control of Cavity Acoustics," AIAA Paper 2000-1927, 2000.
[15] Vakili, A., and Gauthier, C., "Control of Cavity Flow by Upstream Mass-Injection," *Journal of Aircraft*, Vol. 31, No. 1, 1994, pp. 169–174.
[16] Stanek, M. J., Raman, G., Kibens, V., Ross, J. A., Odedra, J., and Peto, J. W., "Control of Cavity Resonance Through Very High Frequency Forcing," AIAA Paper 2000-1905, 2000.
[17] Cattafesta, L. N., Garg, S., and Choudhari, M., "Active Control of Flow-Induced Cavity Resonance," AIAA Paper 1997-1804, 1997.
[18] Baysal, O., Yen, G. W., and Fouladi, K., "Navier–Stokes Computations of Cavity Aeroacoustics with Suppression Devices," *Journal of Vibration and Acoustics*, Vol. 116, No. 1, 1994, pp. 105–112.
[19] Zhang, X., Chen, X. X., Rona, A., and Edwards, J. A., "Attenuation of Cavity Flow Oscillation Through Leading-Edge Flow Control," *Journal of Sound and Vibration*, Vol. 221, No. 1, 1999, pp. 23–47. doi:10.1006/jsvi.1998.2012
[20] Ukeiley, L. S., Ponton, M. K., Seiner, J. M., and Jansen, B., "Suppression of Pressure Loads in Resonating Cavities Through Blowing," AIAA Paper 2003-0181, 2003.
[21] Sarohia, V., "Experimental Investigation of Oscillations in Flows over Shallow Cavities," *AIAA Journal*, Vol. 15, No. 7, 1977, pp. 984–991.
[22] Bauer, R., and Dix, R., "Engineering Model of Unsteady Flow in a Cavity," Arnold Engineering Development Center Technical Rept. AEDCTR-91-17, Dec. 1991.
[23] Kegerise, M. A., Spina, E. F., Garg, S., and Cattefasta, L. N., "Mode-Switching and Nonlinear Effects in Compressible Flow over a Cavity," *Physics of Fluids*, Vol. 16, No. 3, 2004, pp. 678–687. doi:10.1063/1.1643736
[24] Baysal, O., and Stallings, R. L., Jr., "Computational and Experimental Investigation of Cavity Flowfields," *AIAA Journal*, Vol. 26, No. 1, 1988, pp. 6–7.
[25] Zhang, X., and Edwards, J. A., "Computational Analysis of Unsteady Supersonic Cavity Flows Driven by Thick Shear Layers," *The Aeronautical Journal*, Vol. 92, No. 919, 1988, pp. 365–374.
[26] Henderson, J., Badcock, K., and Richards, B. E., "Understanding Subsonic and Transonic Cavity Flows," *The Aeronautical Journal*, Vol. 105, No. 1044, 2001, pp. 77–84.
[27] Kim, I., and Chokani, N., "Navier–Stokes Study of Supersonic Cavity Flow Field with Passive Control," *Journal of Aircraft*, Vol. 29, No. 2, 1992, pp. 217–223.
[28] Alam, M. M., Matsuo, S., Teramoto, K., Setoguchi, T., and Kim, H. D., "A New Method of Controlling Cavity-Induced Pressure Oscillations Using Sub-Cavity," *Journal of Mechanical Science and Technology*, Vol. 21, No. 9, 2007, pp. 1398–1407.
[29] Anon., *FLUENT 6 User's Guide*, Vol. 2, Fluent Inc., Lebanon, NH, 2003, Chap. 10.
[30] Lilly, D. K., "On the Application of the Eddy Viscosity Concept in the Inertial Subrange of Turbulence," National Center for Atmospheric Research Manuscript 123, 1966.
[31] Venkateswaran, S., Weiss, J. M., and Merkle, C. L., "Propulsion Related Flowfields Using the Preconditioned Navier–Stokes Equations," AIAA Paper 92-3437, July 1992.
[32] Lee, Y. K., Raghunathan, S., and Benard, E., "Passive Control of Plume Interference on Axisymmetric Slender Bodies," *AIAA Journal*, Vol. 43, No. 8, 2005, pp. 1653–1662. doi:10.2514/1.2785
[33] Barth, T. J., and Jespersen, D., "The Design and Application of Upwind Schemes on Unstructured Meshes," AIAA Paper 89-0366, 1989.
[34] Jameson, A., Schmidt, W., and Turkel, E., "Numerical Solution of the Euler Equations by Finite Volume Methods Using Runge–Kutta Time-Stepping Schemes," AIAA Paper 81-1259, 1981.
[35] Sakamoto, K., Fujii, K., Tamura, Y., and Matsunaga, K., "Numerical Analysis of a Three Dimensional Cavity Flow Field in a Supersonic Duct," *Transactions of the Japan Society of Mechanical Engineers. Series B*, Vol. 63, No. 606, 1997, pp. 491–496.

J. Oefelein
Associate Editor